TENT5C/FAM46C modulation *in vivo* reveals a trade-off between antibody secretion and tumor growth in multiple myeloma

The *TENT5C/FAM46C* locus on chromosome 1p12 is deleted or mutated in up to 20% of multiple myeloma (MM) patients, revealing a plasma cell (PC)-specific tumor suppressive activity.[1-4] Unlike hitherto known oncosuppressors, TENT5C is not directly involved in DNA repair, cell cycle regulation or apoptosis. In fact, TENT5C is a non-canonical poly(A)polymerase that selectively polyadenylates and stabilizes mRNA encoding immunoglobulins (Ig) and other endoplasmic reticulum (ER)-targeted proteins, exerting a fundamental role in the physiology of PC as intensive antibody producing factories.[5-9] We and others showed that TENT5C specificity for the secretory apparatus requires its association with ER transmembrane FNDC3 proteins, affording TENT5C localization where Ig are translated.[9,10] In this way, TENT5C increases their synthesis, together with that of proteins involved in folding and trafficking along the secretory route, thereby operating as a potent booster of humoral immune response.[9] Accordingly, we found that *TENT5C* is remarkably induced during PC differentiation (*Online Supplementary Figure S1A*), and that its high expression neatly discriminates MM lines from other tumors (Figure 1A). Further strengthening its suppressive role in MM pathobiology, analysis of publicly available genome-scale, pooled CRISPR-Cas9 loss-of viability screens (DepMap portal 23Q2 release) showed that *TENT5C* ablation results in an extremely significant, MM-specific proliferative advantage (Figure 1B). In line with a selective benefit for MM cells in reducing *TENT5C* expression, bone marrow-purified PC from MM patients display lower *TENT5C* expression than those obtained from healthy donors (*Online Supplementary Figure S1B*), with the subset of *TENT5C*-deleted MM patients showing a further decrease in *TENT5C* mRNA levels when compared with non-deleted MM (*Online Supplementary Figure S1C*). We propose that such advantage consists in restricting Ig production and the associated oxidative, metabolic, and degradative workload to save energy for proliferation. Indeed, we showed that TENT5C re-expression in mutated MM lines pushes secretory activity beyond sustainability, inducing ATP shortage, ROS accumulation, and a slower growth rate *in vitro*.[9] However, whether TENT5C regulates the balance between MM growth and antibody secretion *in vivo* remains uninvestigated.

To assess TENT5C impact *in vivo*, we silenced or re-expressed TENT5C in ALMC-2 cells, a MM line expressing the wild-type protein and bearing a hemizygous loss in chromosome 1p,[11] and then injected engineered cells into immunodeficient Rag2$^{-/-}$ IL2rg$^{-/-}$ mice. (Animal procedures were approved by the Italian Ministry of Health and the Institutional Animal Care and Use Committee [IACUC] under protocols 1057 and 1314). Expression of FLAG-tagged TENT5C in ALMC-2 cells significantly increased the abundance of ER mRNA and proteins, and decreased cell proliferation *in vitro* (Figure 1C-F, *Online Supplementary Figure S1D*), inducing cell cycle arrest in G0/G1 phase (*Online Supplementary Figure S1E*). Consistently, TENT5C re-expression had the same effects on proliferation and ER proteins in 3 other TENT5C-deleted MM lines (Figure 1C, *Online Supplementary Figure S1F*).

Conversely, TENT5C-silenced ALMC-2 cells displayed only slight reductions in ER-associated mRNA and proteins (Figure 1D-F, *Online Supplementary Figure S1G*) and no differences in cell growth, viability, and cell cycle distribution (Figure 1C, *Online Supplementary Figure S1D, E*). In general, we found smaller effects of TENT5C silencing in ALMC-2 cells if compared to previously investigated wild-type MM lines,[9] consistent with a pre-existing significant suppression of TENT5C activity in ALMC-2 cells. Importantly, TENT5C was able to promote Ig production and secretion in a dose-dependent manner, with the lowest levels in silenced ALMC-2 cells and the highest in overexpressing counterparts (Figure 1G). Together, these data support a mechanistic link between TENT5C-mediated tumor suppression and its effects on the secretory activity, whereby TENT5C acts as a natural tuner of the secretory capacity of MM cells regulating the trade-off between Ig production and PC proliferation *in vitro*.

To challenge this role *in vivo*, we first injected control, TENT5C-silenced and overexpressing cells intravenously into Rag2$^{-/-}$ IL2rg$^{-/-}$ mice. Despite higher initial circulating Ig light chain (LC) levels (*Online Supplementary Figure S2A*), we found reduced tumor appearance and longer survival in recipients of TENT5C-overexpressing cells (Figure 2A). Indeed, half of the mice in the overexpressing group were still alive and without any sign of disease up to 330 days after injection, while 13 out of 16 mice in the other experimental groups (mock and TENT5C-silenced) had to be sacrificed within 150 days due to the appearance of bulky abdominal plasmacytomas (Figure 2A). Moreover, in line with negative effect of high TENT5C levels on MM proliferation, mRNA and protein analyses on excised plasmacytomas showed significant selection of low TENT5C-expressing cells in the overexpressing group (Figure 2B, *Online Supplementary Figure S2B*). Of note, the only tumor maintaining TENT5C overexpression (lane 11 in Figure 2B) displayed the highest

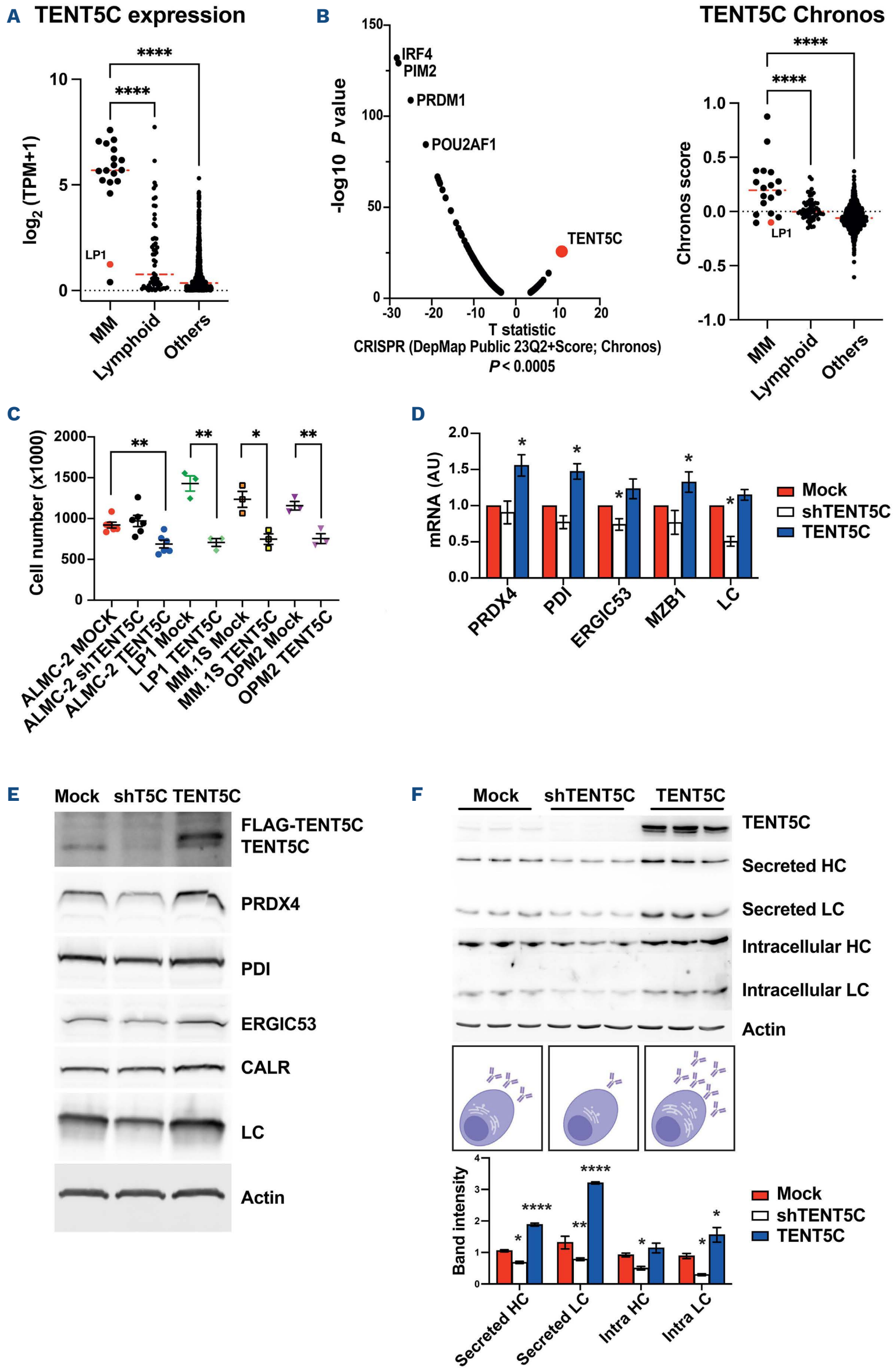

Continued on following page.

Figure 1. TENT5C is a myeloma-specific oncosuppressor that regulates endoplasmic reticulum protein expression and Ig production in a dose-dependent manner. (A) Dot-plot showing *TENT5C* expression in multiple myeloma (MM) *versus* other lymphoid *versus* other cancer cell lines derived from public data available in the DepMap portal (23Q2 release). The full list of 18 myeloma cell lines and of 1,001 non-MM cell lines are available at https://depmap.org/portal/download/all/; LP1 cells, known to harbor a homozygous deletion of *TENT5C*, are highlighted in red (median; ****P<0.0001; one-way ANOVA with Dunnett's multiple comparison). (B) (Left) Volcano plot showing the dependencies enriched in MM cell lines *versus* non-MM cell lines, extracted from DepMap portal 23Q2 release. T statistic and P value for the Chronos dependency scores of the top significant genes (P<0.0005) are shown. A positive T statistic indicates a proliferative advantage of *TENT5C* CRISPR-KO specifically in MM cells. All genetic dependency data, statistical analyses and methods are publicly available in the DepMap portal (23Q2 release). (Right) Dot-plot showing the Chronos dependency score for *TENT5C* in MM *versus* other lymphoid *versus* other cancer cell lines (median; ****P<0.0001; one-way ANOVA with Dunnett's multiple comparison). (C) Equal numbers of MM cells were seeded at $5x10^5$ cells/mL and counted with trypan blue staining after 2 (for ALMC-2, LP1 and MM.1S) or 3 days (for OPM2), (mean ± Standard Error of Mean [SEM]; N=3-6; *P<0.05; **P<0.01; unpaired *t* test *vs.* Mock). ALMC-2 cells were established at relapse as symptomatic MM of a patient initially diagnosed with AL amyloidosis and treated with oral dexamethasone and blood stem cell transplant. ALMC-2 cells bear a t(14;20) translocation, Myc amplification, and p53 deletion. LP1 cells bear a biallelic deletion of *TENT5C* while MM.1S and OPM2 cells a monoallelic deletion and a point mutation on the other allele. All the cell lines were genotyped and *TENT5C* gene was analyzed by Sanger sequencing to confirm wild-type TENT5C expression in ALMC-2 cells and M270V and E178A mutations in MM.1S and OPM2, respectively. Lentiviral viruses to stably express anti-TENT5C or a control shRNA were purchased by Mission shRNA (Sigma-Aldrich, SHC002 and TRCN0000166958). Human C-term FLAG-TENT5C cDNA was purchased by Genscript (OHu30151D) and was cloned in a plasmid with a hybrid bidirectional human PGK-miniCMV promoter co-expressing the protein of interest and truncated human CD271. (D) qRT-PCR analysis of mRNA of selected endoplasmic reticulum (ER)-resident proteins and Ig λ light chain (LC) in TENT5C silenced or overexpressing ALMC-2 cells (mean ± SEM normalized on H3 mRNA; N=4 for silenced, 5 for overexpressed; *P<0.05; Kruskal-Wallis one-way test with Dunn's multiple comparison *vs.* Mock). Total RNA was extracted by lysis in TriFAST (Euroclone, EMR507100). 1000 ng of RNA were retro-transcribed with ImProm-II Reverse Transcriptase System (Promega, A3800). qPCR were performed using iTaq SYBR Green Supermix (Bio-Rad, 1725122) on Bio-Rad CFX96 PCR and analyzed on Bio-Rad CFX Maestro software. Primers are listed in *Online Supplementary Table S1*. (E) Representative immunoblots of selected ER-resident proteins and Ig λ LC in TENT5C silenced or overexpressing ALMC-2 cells. Immunoblots were performed as described by Fucci *et al.*[9] Images were obtained using Uvitec Imager Mini HD9 (Uvitec Ltd.) for HRP-conjugated secondary Ab or FLA9000 (FujiFilm) for Alexa-Fluor conjugated secondary antibodies. Antibodies are listed in *Online Supplementary Table S1*. Band quantifications, performed using ImageJ software (http://rsbweb.nih.gov/ij/), are reported in *Online Supplementary Figure S1G*. (F) Immunoblot analyses of intracellular and secreted IgG λ light (LC) and heavy (HC) chains in TENT5C control, silenced or overexpressing ALMC-2 cells. (Top) Representative blots. (Bottom) Quantifications of intracellular and secreted IgG λ chains (N=3 normalized on actin; *P<0.05; **P<0.01; ****P<0.0001; one-way ANOVA with Dunnett's multiple comparison *vs.* Mock). AU: arbitrary units.

levels of Ig and ER proteins, confirming *in vivo* a dose-dependent effect of TENT5C on the secretory compartment. On the contrary, no selection was detected in TENT5C-silenced tumors that maintained advantageous lower ER and Ig mRNA and protein patterns when compared with control plasmacytomas (Figure 2B, *Online Supplementary Figure S2B*). To timely evaluate the role of TENT5C in modulating the ratio between monoclonal protein and PC proliferation, we then injected TENT5C-overexpressing mice and control ALMC-2 subcutaneously to precisely follow tumor size in a shorter timeframe. We confirmed remarkably reduced tumor growth and longer survival in recipients of TENT5C-overexpressing cells, despite significantly higher circulating LC six days after injection (Figure 2C, D, *Online Supplementary Figure S2C*). At sacrifice, *ex vivo* qRT-PCR and immunoblot analyses showed that TENT5C-overexpressing tumors still displayed higher LC and ER mRNA and protein concentrations than control plasmacytomas (Figure 2E, *Online Supplementary Figure S2D*). Notably, TENT5C abundance significantly modified the ratio between tumor volume and the levels of monoclonal LC concurrently detected in sera (Figure 2F). This *in vivo* association of higher proliferation with decreased secretory activity clearly reveals that loss of TENT5C uncouples monoclonal protein levels from MM burden.

Notably, the impact of TENT5C on secretory products is not restricted to Ig but also promotes the cell surface expression of calreticulin, an ER stress-induced "eat-me" signal, and CD38, an established target of monoclonal antibodies (Figure 3A, B, *Online Supplementary Figure S3E*), with relevant immunotherapeutic implications. Notably, attesting to biological relevance of TENT5C-mediated increase in surface calreticulin, TENT5C-overexpressing ALMC-2 cells underwent increased phagocytosis by primary macrophages *in vitro* (Figure 3C). Moreover, in line with an immunogenic role, qRT-PCR revealed higher expression of monocytic/macrophagic markers (i.e., CD68 and CD206) in TENT5C-overexpressing tumors, indicating larger myeloid infiltrates (Figure 3D), as further confirmed by CD68 immunoblot and immunohistochemistry analyses (Figure 3E, F). In conclusion, our data disclose a trade-off between the sustainable amount of antibodies that PC can produce and their proliferation. TENT5C acts as an "unselfish gene" whose distinctive expression, though inhibitory for PC proliferation, optimizes humoral immunity in favor of the entire organism. Conversely, MM tends to manipulate this equilibrium, blunting TENT5C expression to decrease proteosynthetic activity and favor its own growth. In keeping with this model, loss-of-function mutations have been identified in MM in key transcription factors regulating Ig production and *TENT5C* transcription, namely, *XBP-1* and *PRDM1*.[12] These observations indicate that MM may undergo

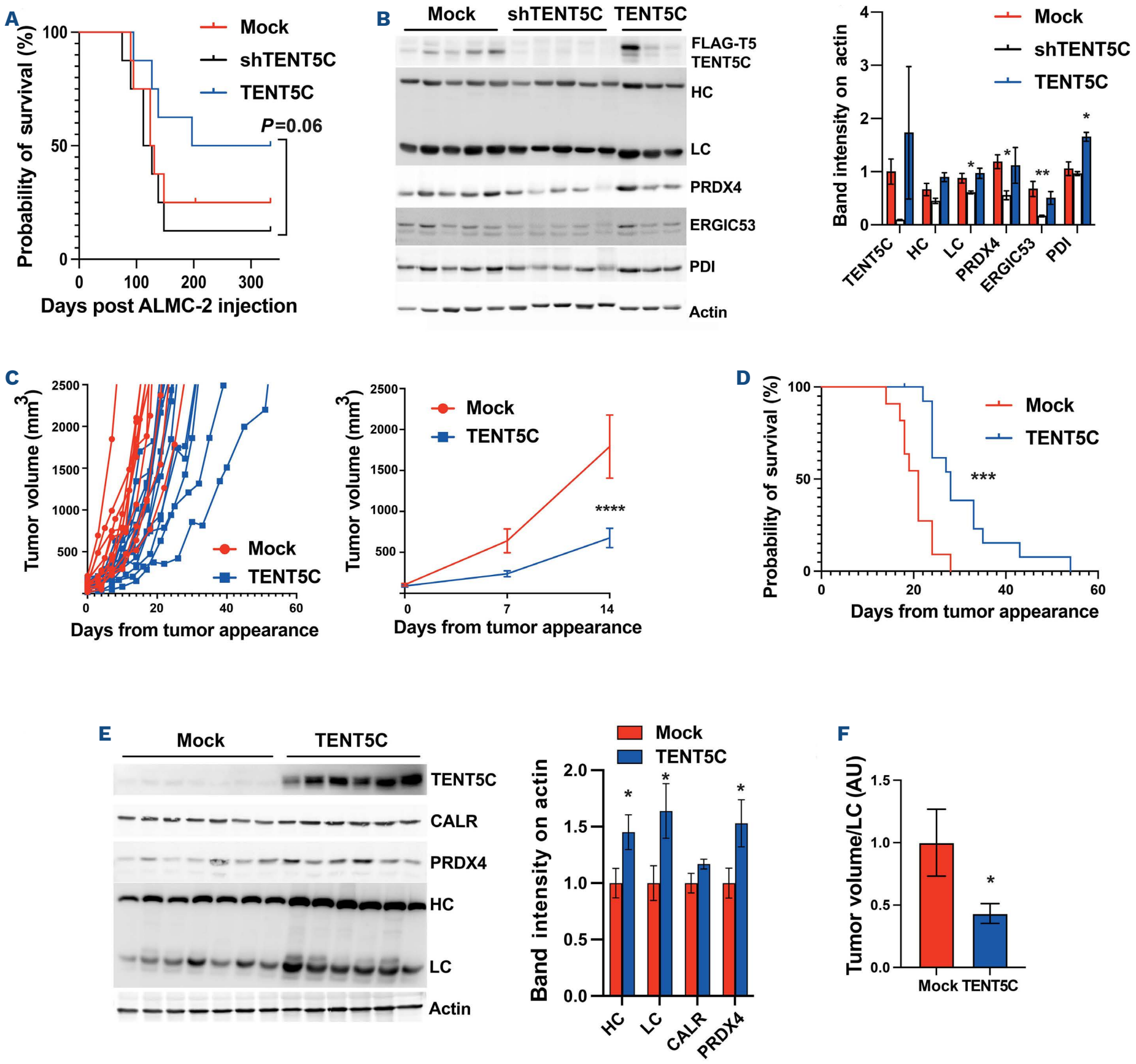

Figure 2. TENT5C regulates the trade-off between antibody secretion and multiple myeloma proliferation *in vivo*. (A) Kaplan-Meier survival curve of male and female 4-6-month-old BALB/c Rag2$^{-/-}\gamma c^{-/-}$ mice intravenously injected in the tail with 10x10^6 control, TENT5C-silenced, overexpressing or control ALMC-2 cells. General health status of the mice was monitored every 3 days and mice were sacrificed at the appearance of lower limb paralysis or abdominal plasmacytomas (N=8 per group; Log-rank Mantel-Cox test). (B) Representative immunoblots of selected ER-resident proteins and IgG λ in excised plasmacytomas formed after intravenous injection. (Left) Immunoblot images. (Right) Band quantifications (mean ± Standard Error of Mean [SEM] normalized on actin; N=5 Mock, 5 shTENT5C, 3 TENT5C; ordinary one-way ANOVA with Dunnett's multiple comparison *P<0.05; **P<0.01; unpaired t test). (C) BALB/c Rag2$^{-/-}\gamma c^{-/-}$ mice were subcutaneously implanted with 3x10^6 ALMC-2 multiple myeloma (MM) cells in the lateral abdominal region. Tumor growth was monitored every 3 days by caliper assessment and mice sacrificed when tumors reached the volume of 2,500 mm^3. Growth of subcutaneous tumors represented individually (left) or as an average (right) in mm^3 ± SEM (N=11 mock, 14 TENT5C; ****P<0.0001; two-way ANOVA with Bonferroni's multiple comparisons). (D) Kaplan-Meier survival curve of mice subcutaneously injected with 3x10^6 control or TENT5C-overexpressing ALMC-2 cells (N=11 Mock, 14 TENT5C; ***P<0.01; Log-rank Mantel-Cox test). (E) Representative immunoblots of selected ER-resident proteins and IgG λ in excised subcutaneous tumors. (Left) Immunoblot images. (Right) Band quantifications (mean ± SEM normalized on actin; N=7 Mock, 6 TENT5C; *P<0.05; unpaired t test). (F) Ratio between the tumor volume measured by caliper and Ig λ LC levels measured by immunoblot in 1 μl of serum collected at the same timepoint (mean ± SEM; N=9 Mock, 10 TENT5C, *P<0.05; unpaired t test). AU: arbitrary units; LC: light chain; HC: heavy chain.

selective pressure to lower, but not completely abolish Ig secretion, suggesting that maintaining Ig production may be beneficial through mechanisms that remain, however, elusive. Moreover, our demonstration that TENT5C modulation uncouples Ig secretion from tumor size may be extremely relevant in MM patients, where, in the presence of TENT5C inactivating mutations, monoclonal protein quantification may underestimate disease burden.

In line with our observation that *TENT5C* loss significantly increases proliferation, inactivating mutations are among the main drivers of evolution from smoldering to active MM.[13] Moreover, deletions of locus 1p, that often include *TENT5C*, are an adverse prognostic factor in MM patients and predict worse responses even to the most active available regimens.[2,14]

Finally, our unprecedented evidence that TENT5C promotes the surface expression of calreticulin and CD38, increasing macrophagic infiltrates, suggests that *TENT5C* mutations may also contribute to reduce MM immunogenicity. In line with this possibility, Maura *et al.*[15] recently found a significant correlation between low *TENT5C* expression and resistance to targeted immunotherapy with the anti-CD38

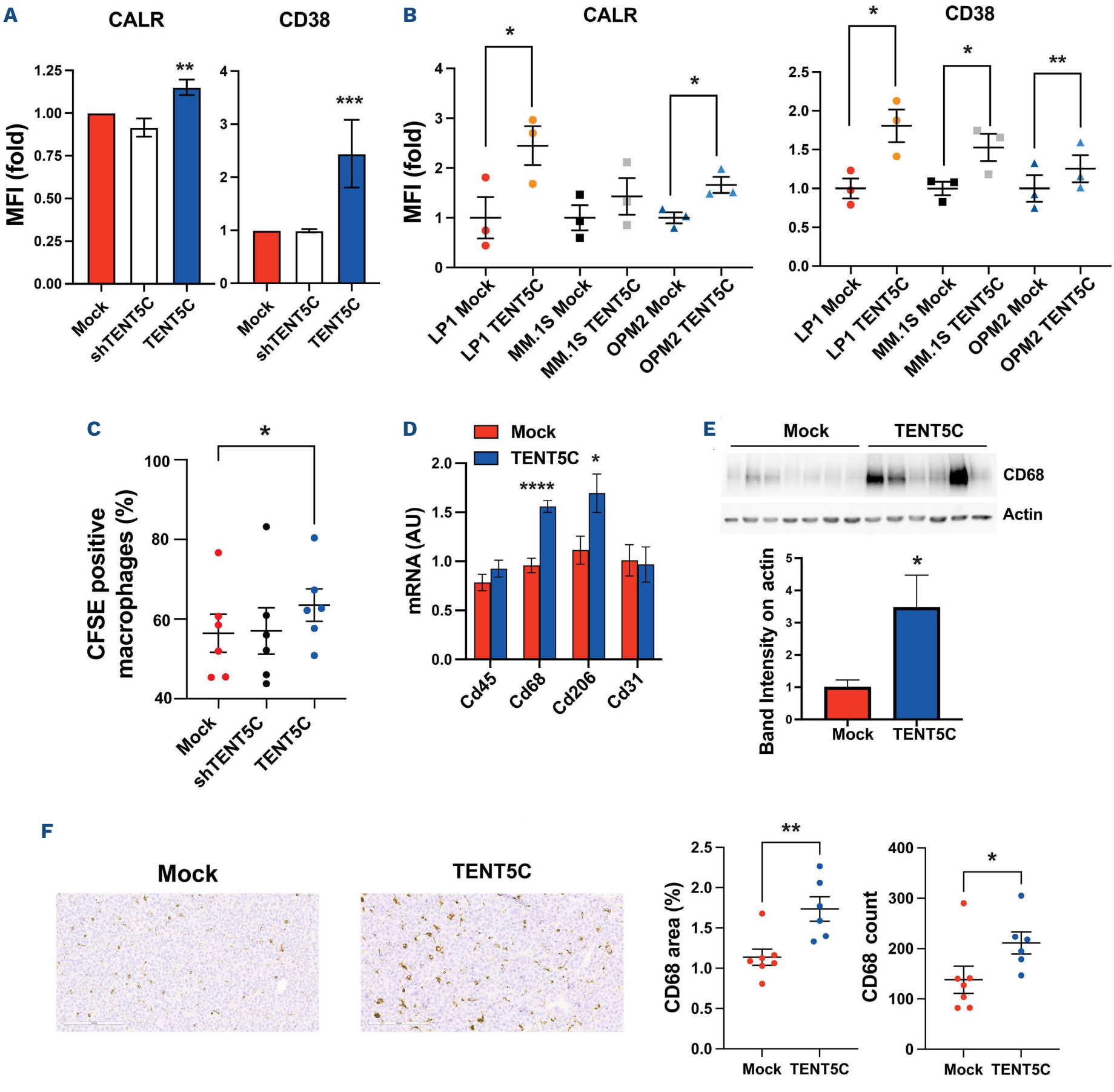

Continued on following page.

Figure 3. TENT5C promotes the expression of calreticulin and CD38 on the cell surface. (A) Cytofluorimetric analysis of CALR and CD38 surface expression in control, TENT5C-overexpressing and silenced ALMC-2 cells (average median fluorescent intensity ± Standard Error of Mean [SEM]; N=18 for CALR and 9 for CD38; ***P*<0.01; ****P*<0.001; Kruskal-Wallis one-way test with Dunn's multiple comparison *vs.* Mock). See *Online Supplementary Figure S2E* for representative cytofluorimetric histograms. Data were obtained with Accuri C6 Flow Cytometer (BD Biosciences) and analyzed using the FCS Express 7 Flow Research Edition (De Novo Software). (B) Cytofluorimetric analysis of CALR and CD38 surface expression in control and TENT5C-overexpressing multiple myeloma (MM) cells (average median fluorescent intensity ± SEM; N=3; **P*<0.05; ***P*<0.01; paired *t* test). (C) Cytofluorimetric analysis of *in vitro* phagocytosis of control, TENT5C-silenced or overexpressing ALMC-2 cells by primary macrophages. Macrophages were obtained by MCSF-induced differentiation of human monocyte purified from the peripheral blood of healthy donors with Pan Monocyte Isolation kit (Miltenyi, 130-096-537). After differentiation, macrophages were stained with 2 μM CellTrace™ Far Red Cell Proliferation kit (Thermo Scientific, C34564). In parallel, TENT5C manipulated ALMC-2 cells were stained with 2 μM CellTrace™ CFSE Cell Proliferation kit (Thermo Scientific, C34544). Stained macrophages and MM cells were mixed 1:1 and incubated at 37°C for 4 hours. The percentage of double positive macrophages was then assessed by BD FACSCanto II (mean ± SEM; N=6; **P*<0.05; repeated measures one-way ANOVA with Dunnett's multiple comparisons *vs.* Mock). (D) qRT-PCR analysis of murine markers in excised subcutaneous tumors (mean ± SEM normalized on GAPDH mRNA; N=7 Mock, 6 TENT5C; **P*<0.05; unpaired *t* test). (E) Immunoblots of murine CD68 in excised subcutaneous tumors. (Top) Immunoblot images. (Bottom) Band quantifications (mean ± SEM normalized on actin; N=7 Mock, 6 TENT5C; **P*<0.05; unpaired *t* test). (F) Immunohistochemistry of murine CD68 in excised subcutaneous tumors. (Left) Representative images: scale bar 200 μm. (Right) Quantifications of CD68 area (%) and counts. Quantification of $CD68^+$ cells was performed with ImageJ software by applying a color threshold on the DAB signal to select positive pixels and analyzing particles (>15 pixels) for area. Area of $CD68^+$ cells was calculated on 4 images/sample (20x magnification), (mean ± SEM; N=7 Mock, 6 TENT5C; **P*<0.05; ***P*<0.01; unpaired *t* test). AU: arbitrary units.

antibody daratumumab. However, since TENT5C may also promote the expression of other membrane molecules and cytokines, further investigations in immunocompetent preclinical models will be required to define the net impact of *TENT5C* loss on MM immunogenicity and sensitivity to immunotherapy.

To summarize, by disclosing the regulation *in vivo* of Ig secretion, MM growth, and the expression of PC surface markers by TENT5C our work advances the understanding of the myeloma-specific role of one of the most frequently mutated oncosuppressors in MM.

Authors

Massimo Resnati,[1] Sara Pennacchio,[1] Lisa Viviani,[1] Tommaso Perini,[1,2] Maria Materozzi,[1] Ugo Orfanelli,[1] Jessica Bordini,[3] Raffaella Molteni,[1] Mario Nuvolone,[4,5] Matteo Da Vià,[6] Francesca Lazzaroni,[6] Niccolò Bolli,[6,7] Simone Cenci[1,8] and Enrico Milan[1,8]

[1]Age Related Diseases Unit, Division of Genetics and Cell Biology, IRCCS San Raffaele Scientific Institute, Milano; [2]Hematology and Bone Marrow Transplantation Unit, IRCCS San Raffaele Scientific Institute, Milano; [3]B-cell Neoplasia Unit, Division of Experimental Oncology, IRCCS San Raffaele Scientific Institute, Milano; [4]Department of Molecular Medicine, University of Pavia, Pavia; [5]Amyloidosis Research and Treatment Center, Fondazione IRCCS Policlinico San Matteo, Pavia; [6]Hematology Unit, Fondazione IRCCS Ca' Granda Ospedale Maggiore Policlinico, Milano; [7]Università degli Studi di Milano, Milano and [8]University Vita-Salute San Raffaele, Milano, Italy

Correspondence:
E. MILAN - milan.enrico@hsr.it

https://doi.org/10.3324/haematol.2023.284299

Received: September 18, 2023.
Accepted: February 13, 2024.
Early view: February 22, 2024.

Disclosures

MN received honoraria from Janssen and research funding from Oncopeptides, Gate Bioscience and Pfizer, and is an inventor on a patent on immunoglobulin sequencing. MDV received funding from GSK and Jannsen (lectures and advisory boards) and Takeda and Amgen (advisory boards). NB received funding from GSK, Janssen, Amgen (honoraria for lectures) and Pfizer (advisory board). The other authors have no conflicts of interest to disclose.

Contributions

MN, SC and EM designed the research. MR, MM, UO, JB, RM, MDV, FL and NB contributed with crucial methodologies and resources. MR, SP, LV, TP and EM performed the experiments and analyzed the data. TP, SC and EM wrote the paper. MN, SC and EM provided the research funds. SC and EM supervised the research.

Acknowledgments

We are particularly grateful to Roberta Colzani for administrative assistance, Paolo Ghia, Diane F. Jelinek, Luca Rampoldi, Emilie Vénéreau, and Ineke Braakman for mice, cells, primers and antibodies, and all the members of the Cenci and Milan labs for fruitful discussions. We thank Amleto Fiocchi and the Animal Histopathology Service at IRCCS San Raffaele Scientific Institute for help with immunohistochemistry analyses. ALMC-2 cells were kindly provided by Diane F. Jelinek, Mayo Clinic, and LP1, MM.1S and OPM2 by Dr. Giovanni Tonon, San Raffaele Scientific Institute. Figure 1G was created using BioRender.com.

Funding

The work was supported by grants to EM from the International Myeloma Foundation (Brian D. Novis Junior Research Award 2019), Fondazione Cariplo Giovani Ricercatori (2018-0257), Fondazione Telethon and Fondazione Cariplo Joint Grant on rare diseases (GJC21079/2022-0577), and to EM and MN from the Italian Ministry of Health (GR-2018-12368387). Additional support came from grants to SC from Fondazione AIRC (IG 23245), the International Myeloma Society (IMS) and Paula and Rodger Riney Foundation (Translational Research Grant 2021 and 2022), and the European Union – Next Generation EU (National Recovery and Resilience Plan, Investment Partenariato Esteso PE8 "Conseguenze e sfide dell'invecchiamento", Project Age-It - Ageing Well in an Ageing Society). MDV was funded by the Umberto Veronesi Foundation and by Pfizer Global Medical Grants (75340503). NB is supported by the European Research Council under the European Union's Horizon 2020 research and innovation program (817997) and Associazione Italiana Ricerca sul Cancro (IG25739).

Data-sharing statement

For original data, please contact: milan.enrico@hsr.it

References

1. Barbieri M, Manzoni M, Fabris S, et al. Compendium of FAM46C gene mutations in plasma cell dyscrasias. Br J Haematol. 2016;174(4):642-645.
2. Boyd KD, Ross FM, Walker BA, et al. Mapping of chromosome 1p deletions in myeloma identifies FAM46C at 1p12 and CDKN2C at 1p32.3 as being genes in regions associated with adverse survival. Clin Cancer Res. 2011;17(24):7776-7784.
3. Bolli N, Biancon G, Moarii M, et al. Analysis of the genomic landscape of multiple myeloma highlights novel prognostic markers and disease subgroups. Leukemia. 2018;32(12):2604-2616.
4. Lohr JG, Stojanov P, Carter SL, et al. Widespread genetic heterogeneity in multiple myeloma: implications for targeted therapy. Cancer Cell. 2014;25(1):91-101.
5. Mroczek S, Chlebowska J, Kuliński TM, et al. The non-canonical poly(A) polymerase FAM46C acts as an onco-suppressor in multiple myeloma. Nat Commun. 2017;8(1):619.
6. Bilska A, Kusio-Kobiałka M, Krawczyk PS, et al. Immunoglobulin expression and the humoral immune response is regulated by the non-canonical poly(A) polymerase TENT5C. Nat Commun. 2020;11(1):2032.
7. Herrero AB, Quwaider D, Corchete LA, Mateos MV, García-Sanz R, Gutiérrez NC. FAM46C controls antibody production by the polyadenylation of immunoglobulin mRNAs and inhibits cell migration in multiple myeloma. J Cell Mol Med. 2020;24(7):4171-4182.
8. Zhu YX, Shi C-X, Bruins LA, et al. Loss of FAM46C promotes cell survival in myeloma. Cancer Res. 2017;77(16):4317-4327.
9. Fucci C, Resnati M, Riva E, et al. The interaction of the tumor suppressor FAM46C with p62 and FNDC3 proteins integrates protein and secretory homeostasis. Cell Rep. 2020;32(12):108162.
10. Manfrini N, Mancino M, Miluzio A, et al. FAM46C and FNDC3A are multiple myeloma tumor suppressors that act in concert to impair clearing of protein aggregates and autophagy. Cancer Res. 2020;80(21):4693-4706.
11. Arendt BK, Ramirez-Alvarado M, Sikkink LA, et al. Biologic and genetic characterization of the novel amyloidogenic lambda light chain–secreting human cell lines, ALMC-1 and ALMC-2. Blood. 2008;112(5):1931-1941.
12. Perini T, Materozzi M, Milan E. The immunity-malignancy equilibrium in multiple myeloma: lessons from oncogenic events in plasma cells. FEBS J. 2022;289(15):4383-4397.
13. Boyle EM, Deshpande S, Tytarenko R, et al. The molecular make up of smoldering myeloma highlights the evolutionary pathways leading to multiple myeloma. Nat Commun. 2021;12(1):293.
14. Odikadze L, Joseph N, Schmidt TM, et al. Outcomes of myeloma patients with deletion 1p receiving lenalidomide, bortezomib, and dexamethasone (RVD) therapy. Blood. 2018;132(Suppl 1):1884.
15. Maura F, Boyle E, Coffey D, et al. Genomic determinants of resistance in newly diagnosed multiple myeloma treated with targeted-immunotherapy. Blood. 2022;140(Suppl 1):1137-1139.